PROCEEDINGS OF SPIE

SPIEDigitalLibrary.org/conference-proceedings-of-spie

Alignment of KB mirrors with at-wavelength metrology tool simulated using SRW

Mourad Idir
Maksim Rakitin
Bo Gao
Junpeng Xue
Lei Huang
Oleg Chubar

SPIE.

Alignment of KB mirrors with at-wavelength metrology tool simulated using SRW

Mourad Idir,[1] Maksim Rakitin,[1] Bo Gao,[2, 3] Junpeng Xue,[1, 4] Lei Huang,[1] and Oleg Chubar,[1]
[1] Brookhaven National Laboratory – NSLS-II, Upton, NY 11973-5000, USA
[2] Shanghai Institute of Applied Physics, Chinese Academy of Sciences, Shanghai 201800, China
[3] University of Chinese Academy of Sciences, Beijing 100049, China
[4] School of Aeronautics and Astronautics, Sichuan University, Chengdu 610065, China

ABSTRACT

Synchrotron Radiation Workshop (SRW) is a powerful synchrotron radiation simulation tool and has been widely used at synchrotron facilities all over the world. During the last decade, many types of X-ray wavefront sensors have been developed and used. In this work, we present our recent effort on the development of at-wavelength metrology simulation based on SRW mainly focused on the Hartmann Wavefront Sensor (HWS). Various conditions have been studied to verify that the simulated HWS is performing as expected in terms of accuracy. This at-wavelength metrology simulation tool is then used to align KB mirrors by minimizing the wavefront aberrations. We will present our optimization process to perform an 'in situ' alignment using conditions as close as possible to the real experiments (KB mirrors with different levels of figure errors or different misalignment geometry).

Keywords: SRW simulation, at-wavelength metrology, X-ray wavefront sensor, X-ray mirror, 'in situ' alignment

1. INTRODUCTION

X-ray mirrors are extensively used both in synchrotron radiation and in table-top laboratory sources in order to collimate or to focus X-ray beams with high efficiency. The improvement in their fabrication technology allows now the manufacturing of quite long X-ray mirrors with rms slope error smaller than 50 nrad, sub-nm rms shape error and with rms roughness smaller than 0.1 nm. Using Kirkpatrick-Baez (KB) geometry, these mirrors can provide diffraction limited spot size smaller than 20 nm at 0.1 nm wavelength [1, 2].

However, reaching this level of spatial resolution obviously requires optimization of the alignment of the whole optical set up and high stability and the mechanical system. In parallel, virtual experiments through computer simulations have gained in popularity in recent years. The results of such simulations reproduce real experiments very well, thus it is becoming easier to make accurate and precise predictions about the outcomes of proposed experiments and to optimize beamline setups to achieve better performance.

The arrangement of two mirrors in a KB configuration [3] is widely used to achieve very small focus sizes reaching the diffraction limit for very short wavelength. In a KB system, the two elliptical cylindrical mirrors are orthogonal to each other and each mirror focuses the X-ray beam in a single plane. In order to reach a diffraction limited spot size, the rms shape errors of the mirrors must be lower than $\lambda/(28\cdot\theta)$ rms where λ is the radiation wavelength and θ is the incidence angle. This level of mirror quality has been demonstrated and the smallest reported beam size is around 13 nm [1].

We have studied mirror alignment of KB optics with the goal of realizing a close loop alignment system using an at wavelength wavefront sensor. In this paper we report the simulation of a Hartmann Wavefront Sensor (HWS) as an instrument to detect aberrations in an X-ray optical system and the way that this HWS can be used to perform close loop alignment. This study was done using the SRW simulation code [4-6].

Advances in Computational Methods for X-Ray Optics IV, edited by Oleg Chubar, Kawal Sawhney, Proc. of SPIE Vol. 10388, 103880Z · © 2017 SPIE
CCC code: 0277-786X/17/$18 · doi: 10.1117/12.2274264

2. X-RAY MIRROR AND HARTMANN WAVEFRONT SENSOR MODELING

In our simulations, the source is located at the origin of the coordinate system and it is modeled as emitting a monochromatic Gaussian X-ray beam with the energy of 9 keV (0.138 nm). The design parameters for the elliptically figured KB mirrors are presented in Table 1.

Table 1: Parameters of KB mirrors in simulation

	VFM	**HFM**
Mirror Length [m]	0.2	0.2
p [m]	50	50.2
q [m]	0.4	0.2
***θ* [mrad]**	3	3

The demagnification ratios are 125 in vertical and 251 in horizontal direction, respectively. Both vertical and horizontal focusing mirrors are elliptical cylinders of length L = 0.200 m with grazing angle θ = 3 mrad at the mirror center. Figure 1 illustrates the optical setup used in our simulation. In the simulation of perfect KB mirrors, we did not add any shape error on the mirror but this can be easily implemented. With the listed parameters from table 1, the expected diffraction limited spot size is about 40 nm×80 nm.

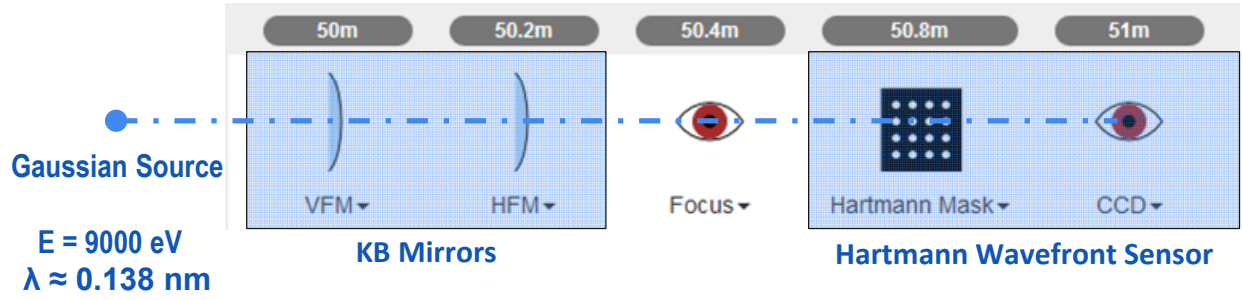

Figure 1. Optical arrangement in wavefront sensing simulation with SRW.

The biggest challenges to obtain nanobeams with KB mirrors are of course the sub-nanometer manufacturing requirements on the substrate shapes but often neglected is the angular alignment and the stability of the mirrors (typically less than few μrad and 10 μrad for, respectively, incidence and orthogonality). Any deviations to these numbers will lead to (spherical) aberrations and astigmatism in the wavefront and to a blurred focus as demonstrated in Figure 2. Several alignment parameters were varied to consider the effect of the misalignments: the glancing angles and the locations of the two mirrors ($\Delta\theta_{VFM}$ = 9.9 μrad, $\Delta\theta_{HFM}$ = -7.0 μrad, ΔZ_{VFM} = 2.3 mm, ΔZ_{HFM} = -1.9 mm). These parameters were selected as a common misalignment of KB optics.

The tolerance limits of the misalignments can be evaluated by comparing the calculated beam size with the diffraction-limited beam size. These different simulated profiles denote that the angle of incidence and the distance between the two mirrors are very important parameters in order to achieve the best focusing condition. Clearly, the glancing angle should be adjusted better than a few μrad.

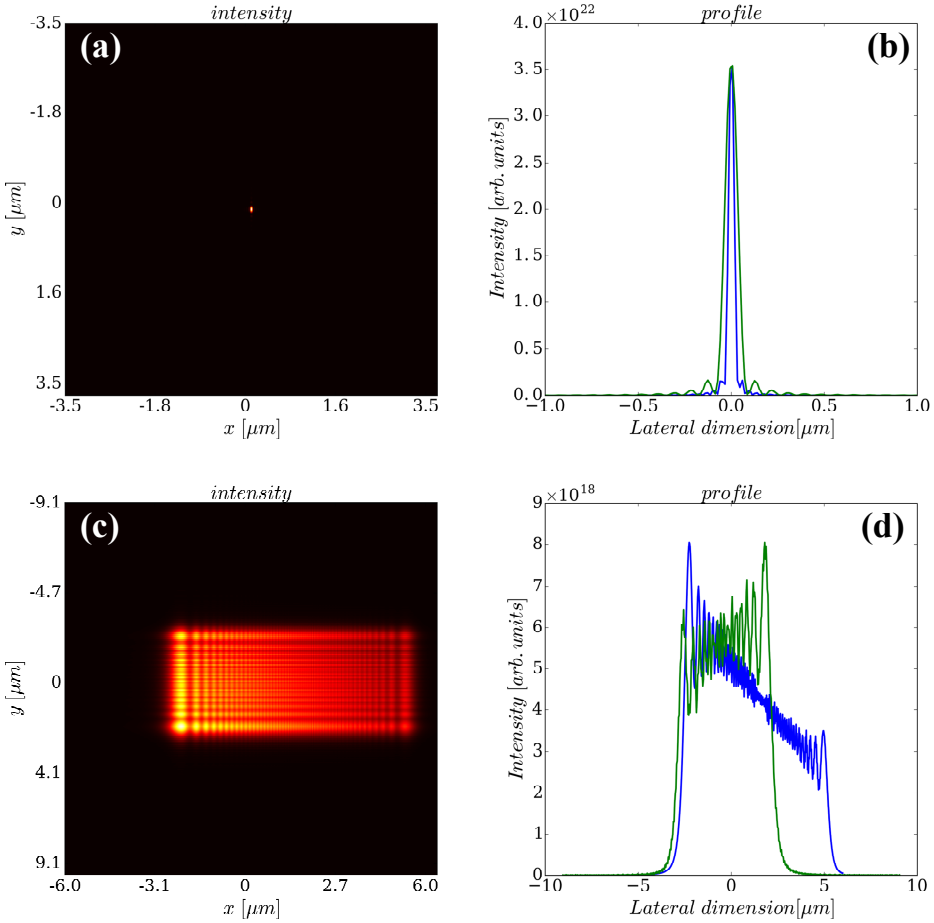

Figure 2. Spot size of perfect KB mirror without alignment error: 2-D distribution (a) and 1-D profiles (b); Spot size of perfect KB mirror with certain alignment error: 2-D distribution (c) and 1-D profiles (d).

Shack-Hartmann wavefront sensors are already successfully applied for real-time wavefront characterization in a wide range of the electromagnetic spectrum from infrared to ultraviolet. These sensors allow for simultaneous measurement of both the phase and intensity distribution. In the Hartmann wavefront sensor technique [7-9], a beam passes through a hole array and is projected onto a CCD camera that detects the beamlet sampled by each hole. The positions of the individual spot centroids are then measured and compared with reference positions. This enables the local slopes of the wavefront (*i.e.* the first derivatives of the wavefront) to be measured at a large number of points within the beam. While Shack-Hartmann wavefront sensors are commonly used for adaptive optics, they have many other applications. The modern Shack-Hartmann wavefront sensor provides information about the optical system performance, including peak-to-valley (PV) wavefront deviation, rms wavefront error, the modulation transfer function (MTF), and the point spread function (PSF). Since the difference between two sets of wavefront is easily computed, the effect of individual optical elements on a complex optical system can be examined.

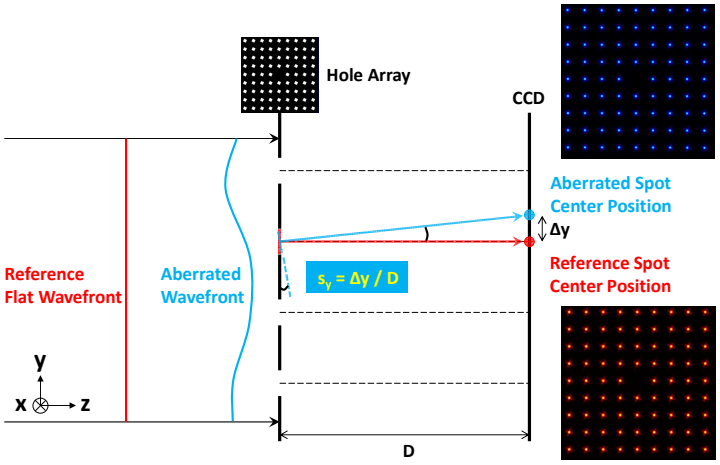

Figure 3. Principle of Hartmann wavefront sensor.

The Hartmann wavefront sensor principle based on an array of holes is shown schematically in Figure 3. The displacement of the spots on the detector is proportional to the wavefront gradient across the corresponding hole in the Hartmann mask. The wavefront can be reconstructed from its gradient data [10, 11].

In our simulation, the Hartmann mask is located at 400 mm from the KB focal spot as illustrated in Figure 1 and consists of an array with 101 × 101 holes (with one hole absent in the center) over a 2 mm × 2 mm area. The holes are squares with 8 μm size, spaced by 20 μm. Each hole is rotated by 25 degrees in order to minimize the overlap of the diffraction patterns from the adjacent holes in the measurement plane. The distance between the grid and the image plane is set to 200 mm. The wavelength is 0.138 nm.

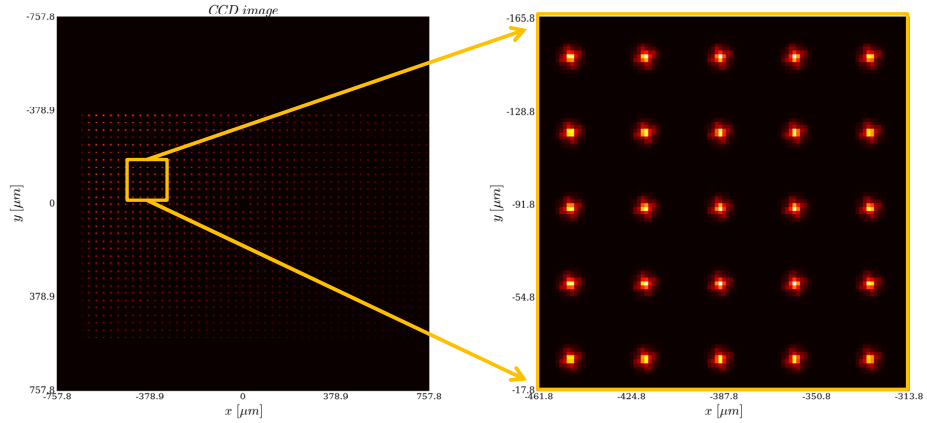

Figure 4. Typical Hartmanngram obtained using SRW.

As pointed out earlier, the importance of alignment of complex optical systems is often underestimated. Alignment of optical systems comprised of even the simplest components can often be a tedious difficult task. For any optics in a system, there are various degrees of freedom commonly used to align an optical system. Misalignments in any of these degrees of freedom will result in optical aberrations. Unfortunately, many of these aberrations are highly coupled, so it is difficult to adjust any one degree of freedom without adversely affecting other parameters. We have designed a new method to quickly decrease aberrations within a complex optical alignment to perform 'in situ' KB mirror alignment. The main idea is to use the mirror motion in combination with a dedicated wavefront sensor. In the example below, we show how to align a KB system in order to obtain minimum of aberrations when trying to reach diffraction limited spot size.

3. LEARNING PROCESS FOR THE INFLUENCE FUNCTIONS AND OPTIMIZATION

The setup in Figure 1 is an example, in which mirrors need to be aligned in order to reduce the main aberrations (astigmatism and coma). We use two degrees of freedom for each mirror. Each degree of freedom modifies the wavefront aberration which can be visualized and measured by the virtual wavefront sensor. As a wavefront sensor, we are using in this virtual experiment is a Hartmann system but any other wavefront sensor type like grating shearing interferometer [12] can be used.

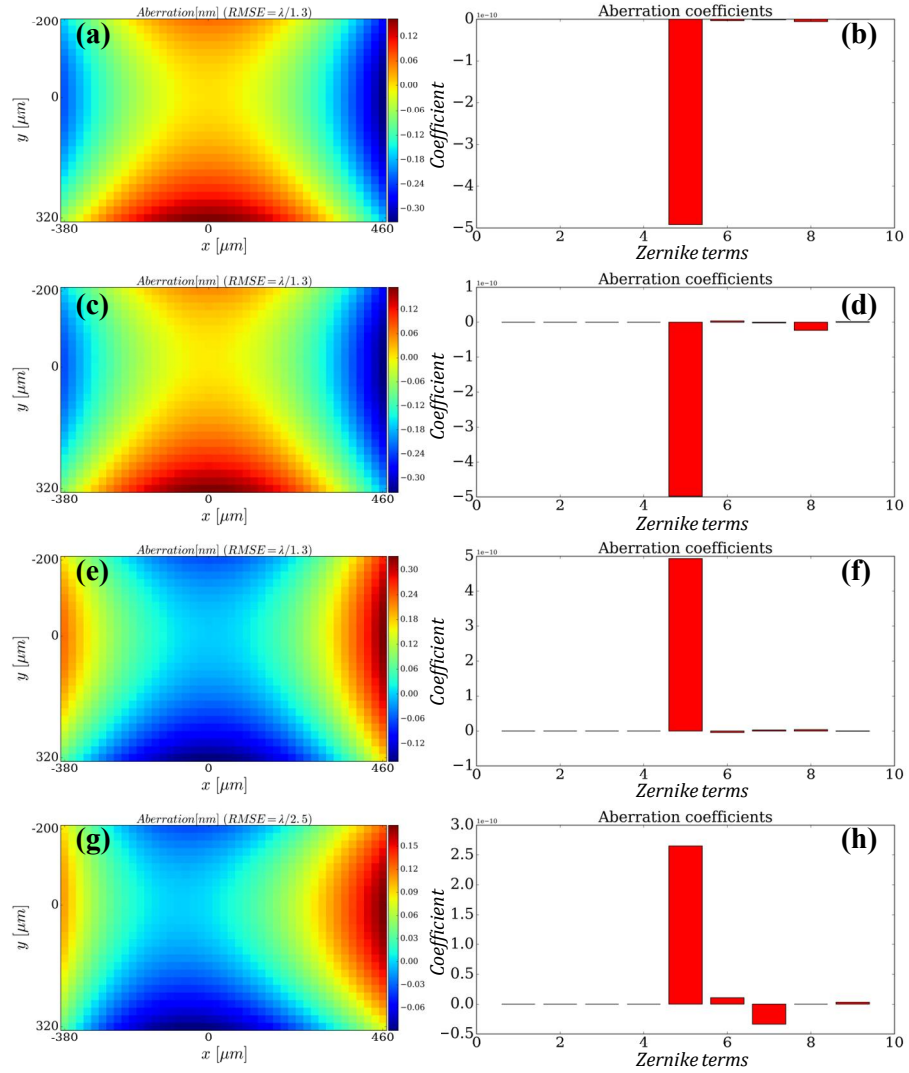

Figure 5. The influence of misalignment:
ΔZ_{VFM} = 1 mm (a) aberration and (b) coefficients; $\Delta\theta_{VFM}$ = 8 μrad: (c) aberration and (d) coefficients;
ΔZ_{HFM} = 1 mm (e) aberration and (f) coefficients; $\Delta\theta_{HFM}$ = 8 μrad (g) aberration and (h) coefficients.

From the simulations shown in Figure 5, we can clearly see that 8 μrad angular errors on the incidence angle or 1 mm offset in the mirror position affect the spot size and generate large aberrations. The main dominant aberrations are astigmatism and coma. Using the simulated wavefront calculated for each actuator motion: translation or angular offset, we can build the influence function matrix. An influence function (IF) measures the effects of small perturbations to the wavefront. This is equivalent to close-loop systems for adaptive optics coupled with wavefront sensor that are often use in astronomy, laser optics or ophthalmology, where wavefront sensors are used to drive adaptive optics to the desired target.

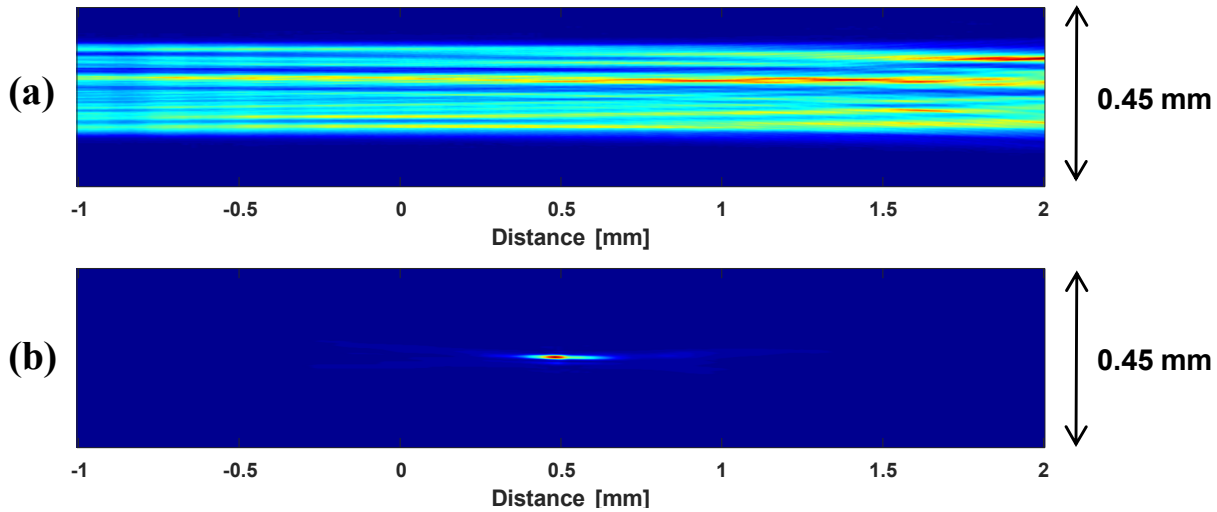

Figure 6. Beam sizes around focus (a) initial state before optimization, and (b) after optimization.

Using this IF matrix, we can build up an interaction matrix and determine the necessary commands to optimize the alignment of the KB mirrors. We added the figure errors less than 1 nm in rms to both KB mirror surfaces (still being wavefront preserving mirrors) in the learning process and optimization. After the optimization, the focus size in Figure 6(b) is highly reduced compared to that of the initial state shown in Figure 6(a). Due to the coupling between different degrees of freedom in the IF, focus location might not be ideally optimized at the nominal position.

4. CONCLUSIONS

The purpose of this research is to demonstrate the power of a wavefront analyzer to perform 'in situ' alignment of a complex X-ray optical system by means of detailed physical optics simulations. Our simulations demonstrate that a Hartmann Wavefront Sensor can be used to 'in situ' align in a close loop diffraction limited KB system. We are developing a dedicated system that will be used in real conditions at X-ray beamlines in the near future.

ACKNOWLEDGEMENTS

This research used resources of the National Synchrotron Light Source II, a U.S. Department of Energy (DOE) Office of Science User Facility operated for the DOE Office of Science by Brookhaven National Laboratory under Contract No. DE-SC0012704.

REFERENCES

[1] Cesar da Silva, J., Pacureanu, A., Yang, Y., Bohic, S., Morawe, C., Barrett, R., and Cloetens, P., "Efficient concentration of high-energy x-rays for diffraction-limited imaging resolution," Optica, 4(5), 492-495 (2017).

[2] Kazuto, Y., Hidekazu, M., Takashi, K., Hirokatsu, Y., Soichiro, H., Satoshi, M., Kenta, A., Yasuhisa, S., Kazuya, Y., Koji, I., Hiroki, N., Jangwoo, K., Kenji, T., Yoshinori, N., Makina, Y., and Tetsuya, I., "Single-nanometer focusing of hard x-rays by Kirkpatrick–Baez mirrors," Journal of Physics: Condensed Matter, 23(39), 394206 (2011).

[3] Kirkpatrick, P., and Baez, A. V., "Formation of Optical Images by X-Rays," Journal of the Optical Society of America, 38(9), 766-774 (1948).

[4] Chubar, O., and Elleaume, P., "Accurate and efficient computation of synchrotron radiation in the near field region." Conf. Proc., 6th European conference, EPAC98, Vol. 1-3, 1177-1179.

[5] Chubar, O., Elleaume, P., Kuznetsov, S., and Snigirev, A., "Physical optics computer code optimized for synchrotron radiation." Proc. SPIE 4769, 145-151.

[6] Chubar, O., Fluerasu, A., Berman, L., Kaznatcheev, K., and Wiegart, L., “Wavefront propagation simulations for beamlines and experiments with "Synchrotron Radiation Workshop",” Journal of Physics: Conference Series, 425(16), 162001 (2013).
[7] Tarabocchia, M., and Holly, S., "Dynamic Hartmann wavefront sensor in applications." 343, 93-100.
[8] Mercère, P., Idir, M., Zeitoun, P., Levecq, X., Dovillaire, G., Bucourt, S., Douillet, D., Goldberg, K. A., Naulleau, P. P., and Rekawa, S., “X ray Wavefront Hartmann Sensor,” AIP Conference Proceedings, 705(1), 819-822 (2004).
[9] Abraham, E., Cahyadi, H., Brossard, M., Degert, J., Freysz, E., and Yasui, T., “Development of a wavefront sensor for terahertz pulses,” Optics Express, 24(5), 5203-5211 (2016).
[10] Huang, L., Idir, M., Zuo, C., Kaznatcheev, K., Zhou, L., and Asundi, A., “Comparison of two-dimensional integration methods for shape reconstruction from gradient data,” Optics and Lasers in Engineering, 64, 1-11 (2015).
[11] Huang, L., Xue, J., Gao, B., Zuo, C., and Idir, M., “Spline based least squares integration for two-dimensional shape or wavefront reconstruction,” Optics and Lasers in Engineering, 91, 221-226 (2017).
[12] Weitkamp, T., Diaz, A., David, C., Pfeiffer, F., Stampanoni, M., Cloetens, P., and Ziegler, E., “X-ray phase imaging with a grating interferometer,” Optics Express, 13(16), 6296-6304 (2005).